JOURNAL OF MATERIALS SCIENCE 9 (1974) 129–135

Application of fracture mechanics to plastics deformed at high strain-rates

P. E. REED, H. V. SQUIRES
Department of Materials, Queen Mary College, University of London, UK

Thin walled cylindrical specimens of poly(methylmethacrylate) containing artificial flaws of different length and machined along a generator of the cylinder, are subjected to internal pressure pulses (shock pulses) of increasing magnitude until fracture occurs. A shock tube is used to generate the shock pulse. The variation of the stress required to induce fracture with crack length is studied. It is found that an equation similar to the Griffith relationship applies over the range of crack lengths 38 mm > 2 c > 16 mm, the surface energy value required to fit the Griffith type equation to the experimental data in this crack length range being similar to that derived from quasi-static testing of the same material. It is found that the range of applicability of the Griffith equation is determined by the magnitude of the fracture stress of the non-artificially flawed material at the particular strain-rate at which the test is conducted.

1. Introduction

Griffith's [1] expression relating the fracture stress, σ_f, and semi-crack length, c, for a crack contained in an infinite plate subjected to uniaxial stress at infinity, perpendicular to the plane of the crack is

$$\sigma_f = \left[\frac{2E\gamma}{\pi c}\right]^{\frac{1}{2}} \quad (1)$$

where E is the elastic modulus for the material and γ the specific surface energy.

Attempts to apply this equation to the fracture of many polymeric materials has shown that a relationship of the form

$$\sigma_f = A\,c^{-\frac{1}{2}} \quad (2)$$

holds in many instances, but that the value of the constant A differs considerably from that predicted by Griffith. In particular, the magnitude of the surface energy required to fit the equation to experimental data is much larger than is theoretically possible from elastic considerations alone [2]. The linearly proportional relationship between fracture stress and square root of the crack length has been shown to apply to the fracture of glassy plastics under different loading conditions [3-5]. In these experiments, either an edge crack or an internal crack was used in a uniaxial stress system as required for application of the Griffith theory. A further feature of the previous experimental work cited, is that the rate of load application was quasi-static.

Attempts have been made to apply fracture mechanics to problems associated with rapid application of load [6], i.e. under impulsive loading. The traditional laboratory tests for investigating impulsive loading of materials are the Izod and Charpy impact tests. In each of these tests a short beam specimen containing an edge notch is struck by a swinging hammer to induce fracture. Since the specimen is fractured in bending in these standard impact tests, the stress field within the specimen well away from the notch is non-uniform. Hence the stress field of specimens in standard impact tests varies from the uniform stress field assumed in Griffith's original analysis which complicates data interpretation. A further complication in standard impact testing is that an oscillatory loading pattern can occur if the stiffness of the striking hammer is not matched to the stiffness of the specimen [6, 7].

An alternative method of impact testing utilizes a shock tube to deliver the impulsive load to the specimen [8]. The specimen in this case is a thin walled cylinder, through which the shock pulse passes causing sudden application of an internal pressure to the specimen. Loading in this manner leads to the entire specimen being

uniformly loaded within a very short time interval. A second advantage is that a higher strain-rate can be achieved with a shock tube (10^3 sec^{-1}) than in swinging hammer tests. The loading rate at a shock front is essentially infinite and the limitations on strain-rate are, therefore, those imposed by the specimen being tested and the strain measuring system. Ideally, the only stress acting on the specimen after application of the pressure is the hoop stress. Hence specimens containing axial cracks, machined along a generator of the cylinder, may be compared with the uniaxial tensile specimens used by Berry [2]. The major difference in the two stress systems is the presence of bending moments in the case of the cylinder, owing to the action of the internal pressure near the crack edges, tending to rotate the crack edges out of the plane of the hoop stress. This bending moment reduces the hoop stress otherwise required to cause failure and increases in magnitude with the crack length [5].

2. Experimental

The general shock tube test assembly is shown schematically in Fig. 1. It consists of a driver and driven section (i.d. 42.4 mm), a double diaphragm section and a dump tank containing the specimen clamping fixture. The dump tank acts as a pressure vessel extension of the shock tube and also serves to contain the fragments of fractured specimens. The cylindrical specimens are mounted to form an extension of the driven section within the dump tank.

Fig. 2 shows the method of holding the specimens. Axial clamping between two end plates has been employed, the clamping pressure being just sufficient to prevent the specimen from falling under its own weight. Two knife edge lips on the end plates are provided for specimen location, the bore of the specimen forming a continuous and smooth wall with the driven section. By this method the specimen is virtually a freely suspended body free to expand radially throughout its length except for a small frictional force acting on its ends.

To perform an impact test, the pressures of the driver and driven gases, nitrogen and air respectively, are adjusted so as to generate a shock pulse of the required magnitude. A double diaphragm system was used to aid in obtaining a precisely controlled shock pressure. On rupturing the diaphragms in the usual manner [9, 10], the shock passes along the driven section and through the specimen causing it to fracture when the shock pressure is sufficiently high.

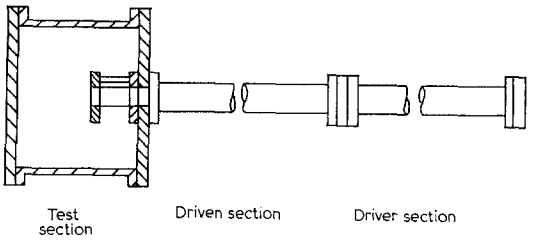

Figure 1 Schematic drawing of shock tube test assembly.

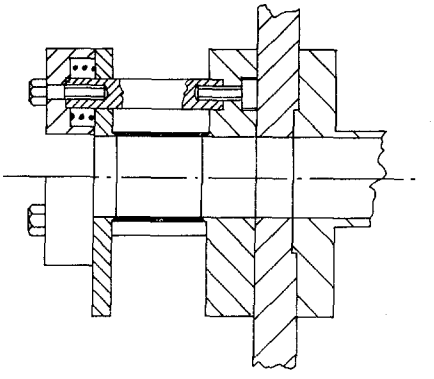

Figure 2 Schematic drawing of specimen mounting arrangement.

The thin walled cylindrical specimens used were of length 50.8 mm, wall thickness 0.762 mm and 42.4 mm i.d. to match the bore of the shock tube. The specimen length of 50.8 mm was always less than the length of the shock pulse, i.e. the length of the travelling high pressure gas zone between the shock front and the following rarefaction wave. The specimen length thus satisfied the condition that the whole specimen be subjected to uniform internal pressure until fracture occurred. The specimens were machined from commercially produced poly(methylmethacrylate) (PMMA) extruded tube. Chamfers to suit the knife edge lips on the supporting plates were machined into the bore at the ends of each specimen for location purposes.

Cracks of the desired length were produced in the walls of the tubular specimen by drilling through the wall at one end of the required crack and then traversing the drill along a generator of the cylinder to cut the crack to the required length. Production in this manner produced blunt-ended cracks with tip radii of 0.38 mm. Sharp-ended cracks were produced

in the same manner by additionally inserting a razor blade at each end of the crack. Specimens were produced with blunt- or sharp-ended cracks of various lengths in the range 0.76 to 38 mm, each crack being centrally located along the generator of the tube.

Each specimen was mounted in the specimen holder within the dump tank and subjected to a series of shock pulses of steadily increasing pressure until fracture occurred. The test was thus a go/no-go test by which the minimum pressure required to cause fracture was ascertained.

The shock pressure, P_2, was calculated from measurements of the driver gas pressure, P_4, and driven gas pressure, P_1, using the relationships [9, 10]

$$\frac{P_4}{P_1} = \frac{2\gamma_1 M^2 - (\gamma_1 - 1)}{(\gamma_1 + 1)} \left\{1 - \frac{(\gamma_4 - 1)}{(\gamma_1 + 1)} \frac{a_1}{a_4}\left[M - \frac{1}{M}\right]\right\}^{\frac{-2\gamma_4}{\gamma_4 - 1}} \tag{3}$$

$$\frac{P_2}{P_1} = \frac{2\gamma_1 M^2 - (\gamma_1 - 1)}{\gamma_1 + 1} \tag{4}$$

where γ_1 and γ_4 are the ratios of specific heats of the driven and driver gas respectively, a_1 and a_4 are the velocities of sound in the driven and driver gas respectively, and M is the shock Mach number.

Shock pulse pressures were converted to hoop stress, σ_θ, using the expression

$$\sigma_\theta = P_2 R/t \tag{5}$$

where R and t are the mean radius and wall thickness of the specimen.

The expression for hoop stress is that derived from equilibrium considerations of a statically loaded thin walled cylinder subjected to internal pressure, P_2. Although such conditions do not exist under shock loading, it has been shown [11] that this expression does not lead to serious errors even under impulse loading.

3. Results and discussion

Figs. 3 and 4 show, for blunt and sharp cracks respectively, the variation of the fracture stress, σ_θ (calculated using Equation 5) versus $(2c)^{-\frac{1}{2}}$. According to Griffith's theory (Equation 1) or generalized flaw theory (Equation 2) there should be a linear relationship between σ_θ and $c^{-\frac{1}{2}}$, with $\sigma_\theta \to 0$ when $c^{-\frac{1}{2}} \to 0$. In Figs. 3 and 4 all test results have been plotted, the circles represent tests in which fracture of the specimen did not occur, while the squares represent the pressure, or stress, that the particular specimen had to be subjected to in order to cause fracture. Some specimens with short cracks did not fail on the first loading series but were found to fracture at a stress lower than the maximum previously sustained in a subsequent series. Such reductions may be a consequence of the loading history or other undetermined ageing effects. Also included in Figs. 3 and 4 are Berry's data [2] for the fracture of flawed flat plates of poly(methylmethacrylate) containing edge notches of length c, subjected to quasi-static uniaxial stress.

A linear relationship exists between the calculated minimum hoop stress required for fracture, σ_f, and $(2c)^{-\frac{1}{2}}$ for large crack lengths in the ranges $0.16 < (2c)^{-\frac{1}{2}} < 0.28$ mm$^{-\frac{1}{2}}$ (i.e. 38 mm $> 2c >$ 12.7 mm) for blunt cracks and $0.16 < (2c)^{-\frac{1}{2}} < 0.4$ mm$^{-\frac{1}{2}}$ for sharp cracks. This relationship may be expressed as

$$\sigma_\theta = \sqrt{\left(\frac{2E\gamma}{\pi c}\right)} - \sigma_\infty.$$

The data in this region deviates only slightly from Berry's data for quasi-static loading in the case of sharply notched specimens. Using a value of 2.93 GN m^{-2} for the elastic modulus

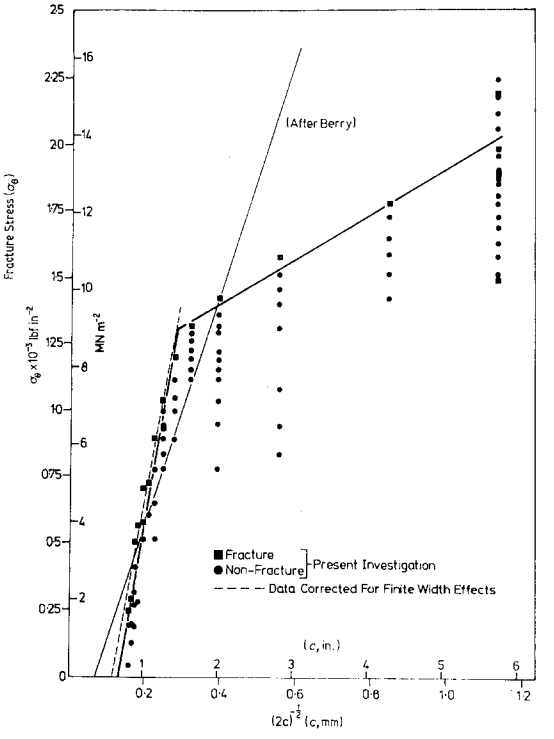

Figure 3 Fracture stress data for blunt cracks.

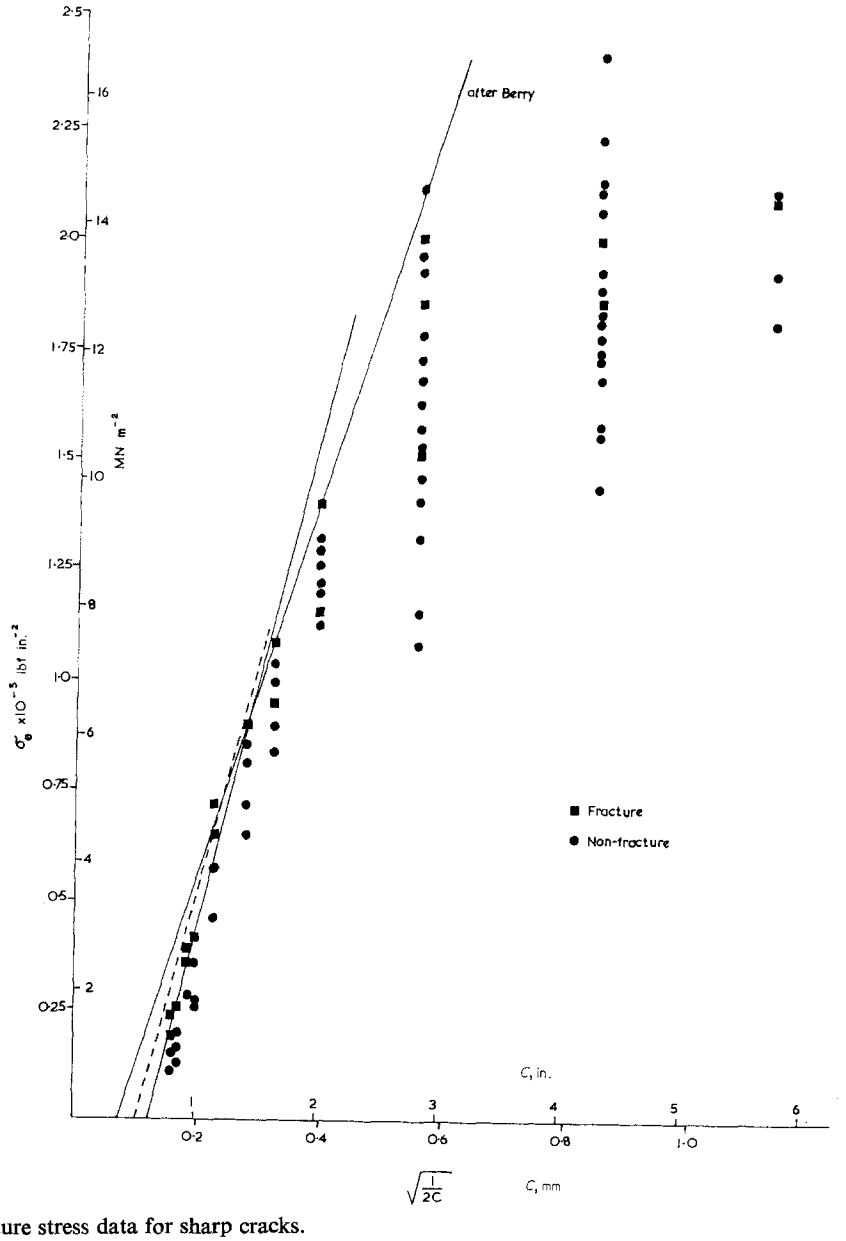

Figure 4 Fracture stress data for sharp cracks.

leads to values of 8.6×10^2 and 4.2×10^2 J m^{-2} for the surface energy (γ) for blunt and sharp cracks as calculated from the Griffith type equation. These values differ only by a factor of 1.5 to 3 from that calculated by Berry of 3.0×10^2 J m^{-2} for quasi-static testing of PMMA in uniaxial tension.

Although a linear relationship exists between σ_f and $(2c)^{-\frac{1}{2}}$, the curves for the large crack length regions previously discussed do not extrapolate to the origin as required to fit the Griffith equation. Corrections of the fracture stress data for finite width and bending effects have been ignored in the previous analysis. Ratios of crack length/"plate" width reach 0.75 for the largest crack lengths used. Clearly, finite width effects will be present reducing the stress required to cause failure. The stress intensity factor, K, for a uniaxially stressed plate of width w containing a crack of length $2c$ is [13]

$$K = \sigma_f \left[w \tan\left(\frac{\pi c}{w} \right) \right]^{\frac{1}{2}}. \quad (6)$$

For an infinitely wide plate this reduces to

$$K = \sigma_i (\pi c)^{\frac{1}{2}}. \quad (7)$$

Hence, the correction factor to be applied to the fracture stress measured for the effect of finite width is

$$\left[w \tan\left(\frac{\pi c}{w} \right) / \pi c \right]^{\frac{1}{2}}$$

and leads to the dotted lines shown in Figs. 3 and 4. The surface energy values corresponding to these lines are 8.2×10^2 and 3.2×10^2 J m^{-2} for blunt- and sharp-ended cracks respectively and the constant σ_∞ is reduced by this correction.

Folias [14] and Williams and Ewing [5] have studied the application of fracture mechanics to internally pressurized cylinders containing axial cracks. The analysis, considering both tension and bending effects, leads to the form for the stress intensity factor

$$K = \sigma_\theta \sqrt{(\pi c)} \left(1 + 1.67 \frac{c^2}{Rt} \right)^{\frac{1}{2}} \quad (8)$$

where R is the cylinder radius, t the wall thickness and σ_θ the hoop stress. The bending effect thus causes the hoop stress for fracture to be a factor of $(1 + 1.67\, c^2/Rt)^{\frac{1}{2}}$ less than the uniaxial stress required for fracture in the equivalent flat plate. Fig. 5 shows the variation of equivalent flat plate fracture stress with crack length (i.e. the σ_θ fracture values from Figs. 3 and 4 modified by the finite width and bending correction factors). The form of the curves in Fig. 5 is unusual and casts doubt on the applicability of the bending correction factor to thin walled cylinders at high straining rates.

When the crack lengths are short ($2c < 16$ mm, $(2c)^{-\frac{1}{2}} > 0.24$ mm$^{-\frac{1}{2}}$) the fracture stress data obtained from high strain-rate testing deviates from the previously discussed linear relationship for large cracks. For blunt-ended short cracks (Fig. 3) a linear relationship between σ_θ and $(2c)^{-\frac{1}{2}}$ was observed initially but clearly the Griffith equation cannot meaningfully be applied in this region. Subsequent testing on sharp- and blunt-ended cracks showed considerable scatter in the fracture stress data of short crack length specimens. It is most likely that the fracture stress when $(2c)^{-\frac{1}{2}} > 0.24$ mm$^{-\frac{1}{2}}$ ($2c < 16$ mm) is independent of artificial flaw size. This view is supported by one test in which a fragment of the shattered specimen after testing was found to contain the artificially machined sharp crack. Fracture had initiated everywhere but at the artificial crack in this case.

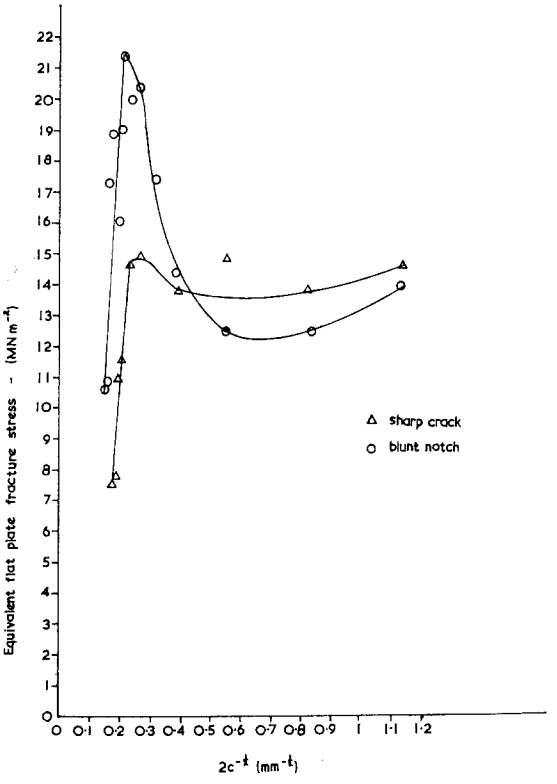

Figure 5 Fracture stress data after correcting for bending effects.

The mode of fracture of specimens having long artificial cracks ($2c > 16$ mm, $(2c)^{-\frac{1}{2}} < 0.24$ mm$^{-\frac{1}{2}}$) differs from that obtained with specimens having shorter cracks. When the crack is long ($2c > 16$ mm) the specimen fails by the propagation of single cracks from the flaw tips as shown in Fig. 6. This mode of failure is identical to that found in quasi-static testing of the same material. Examination of fracture surfaces of specimens which fail in this manner (Fig. 7) verifies that fracture initiates at the root of the artificial crack and propagates towards the ends of the cylinder. When the crack length is small ($2c < 16$ mm), specimen failure occurs by gross fragmentation. Failure in this case is probably initiated at numerous points throughout the specimen and not at the artificial crack tips.

The transition in fracture mode coincides approximately with the abrupt change in slope of the σ_θ versus $(2c)^{-\frac{1}{2}}$ data for blunt-ended

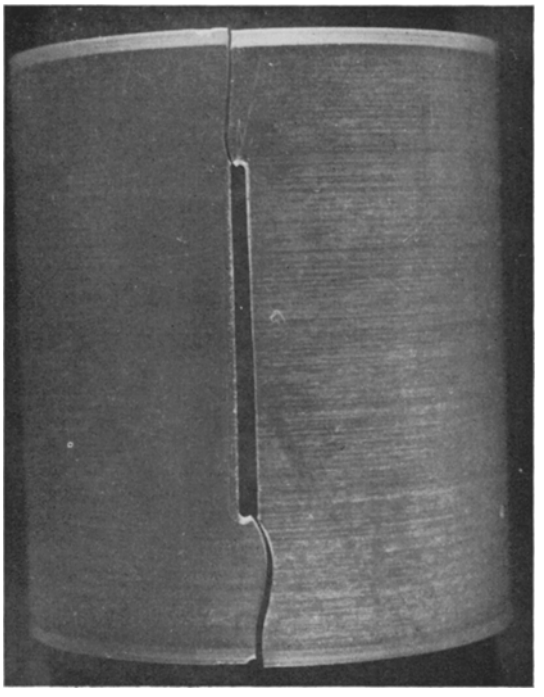

Figure 6 Specimen failure by the propagation of a single crack.

cracks only (Fig. 3) and coincides exactly with the maxima on the equivalent flat plate fracture stress data (Fig. 5) for both blunt and sharp cracks. This behaviour is invariant with the position of the artificial flaw on the generator of the cylindrical specimen. Fracture mechanics can only be applied when fracture initiates and propagates from a crack of known size and position in the stress field, since the theories always contain a crack length term. When shattering occurs and fracture is initiated at an unknown flaw, applications of the Griffith equation and corrections for finite width and bending utilizing the artificial flaw length are not justified. Thus the values of σ_θ (Figs. 3 and 4) when $(2c)^{-\frac{1}{2}} > 0.24$ mm$^{-\frac{1}{2}}$ are not amenable to analysis by the Griffith equation and the equivalent flat plate fracture stress values for the same crack length range (Fig. 5) derived from Equation 8 have little significance. When $2c < 16$ mm the hoop stress for fracture is less than that required according to the Griffith equation and is independent of artificial flaw size.

At the high strain-rates used in the present tests, the Griffith type relationship can be meaningfully applied only to specimens containing crack lengths in the range 38 mm $> 2c > 16$ mm ($0.16 < (2c)^{-\frac{1}{2}} < 0.24$ mm$^{-\frac{1}{2}}$). The effect of tube length on this range may be a factor in determining the extent of this crack length range. Since the σ_θ versus $(2c)^{-\frac{1}{2}}$ plot does not pass through the origin as required to fit the Griffith equation, it appears that the correction factors applied are inadequate. Applying the bending correction factor leads to surface energy values of 8.5×10^3 and 3.7×10^3 J m^{-2} for blunt- and sharp-ended notches respectively for the crack length range 38 mm $> 2c > 16$ mm. These values are an order of magnitude greater than values previously quoted for PMMA for a range of crack speeds [15]. At the high strain-

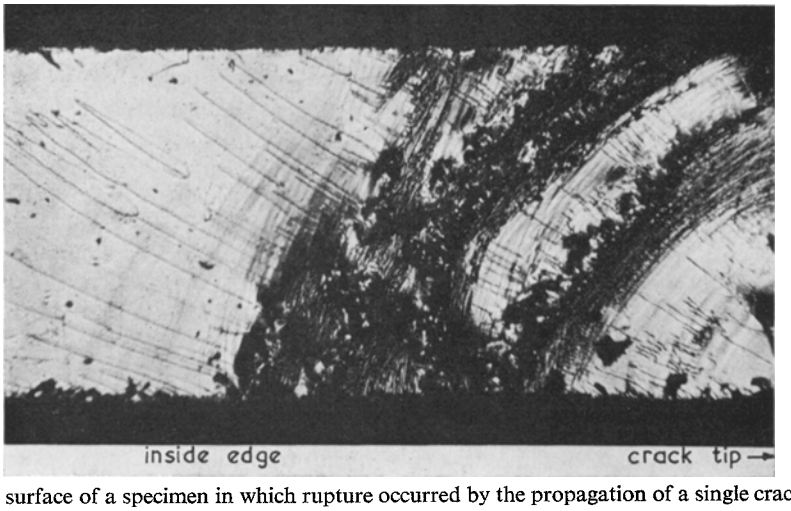

Figure 7 Fracture surface of a specimen in which rupture occurred by the propagation of a single crack. (The tip of the artificially induced flaw is to the right of the photomicrograph.) × 60.

rates of the present tests, it is possible that the time scale of the experiment is insufficient for bending in the vicinity of the crack to reach equilibrium position. Smaller deflections lead to low bending stresses and the bending correction factor used will be too large since it is based on equilibrium considerations. This may account for the unusually high surface energy values after application of the bending correction factor.

It has been shown [12] that the fracture stress of PMMA decreases with increasing strain-rate when the present high strain-rates are used. Non-artificially flawed cylindrical specimens tested under quasi-static internal pressurization fracture at a hoop stress of 40 MN m^{-2} and at 16 MN m^{-2} under shock loading conditions. It can be seen from Fig. 4 that the hoop stress at fracture for specimens containing short crack lengths is approximately the same as for non-artificially flawed samples. The transition in fracture mode from single crack propagation to shattering may thus be related to the hoop stress approaching a critical value rather than being governed by the flaw size as previously suggested.

4. Conclusion

The hoop stress (σ_θ) to fracture thin walled cylinders of PMMA containing axial cracks by the application of a step functional pressure pulse obeys the equation

$$\sigma_\theta = \frac{p R}{t} = \sqrt{\left(\frac{2 E \gamma}{\pi c}\right)} - \sigma_\infty$$

(where σ_∞ is a constant) either over a limited range of crack length (38 mm $> 2c >$ 16 mm) or provided σ_θ is less than a critical value which causes the tube to shatter. σ_θ is independent of crack length when shattering occurs. When the Griffith type equation is obeyed, fracture occurs by the propagation of single cracks normal to the major principal stress from the artificially inserted flaw. Values of surface energy required to fit the above equation to the high strain-rate fracture data are found to be similar to those quoted for quasi-static testing of the same material after the data are corrected for finite width effects. Attempts to correct the data further for bending effects using the Folias relationship[14], eliminate the constent σ_∞ and fit the data to a true Griffith equation, have been unsuccessful. It is considered that the high strain-rates used in the present tests reduce the bending effect because of the short time scale of the experiment and that the correction factor employed overestimates the bending effect.

Acknowledgement

The authors gratefully acknowledge the financial assistance given by the Ministry of Defence and the Science Research Council in connection with this project.

References

1. A. A. GRIFFITH, *Phil. Trans. Soc.* **A221** (1921) 163.
2. J. P. BERRY, *J. Polymer Sci.* **50** (1961) 107.
3. B. ROSEN, "Fracture Processes in Polymeric Solids" (Wiley, New York, 1964).
4. J. J. BENBOW and F. C. ROESLER, *Proc. Phys. Soc. (London)* **B70** (1957) 201.
5. J. G. WILLIAMS and P. D. EWING, 2nd International Conference on Fracture, Brighton, "Fracture 1969" (Chapman and Hall, London, 1969).
6. C. E. TURNER, L. E. CULVER, J. C. RADON and P. KENNISH, *J. Inst. Mech. Eng.* **38** (1971) 38.
7. J. C. RADON and C. E. TURNER, *Eng. Frac. Mech.* **1** (1969) 411.
8. E. H. ANDREWS, L. BERNSTEIN, P. J. NURSE and P. E. REED, Proceedings of the 8th International Shock Tube Symposium, "Shock Tube Research" (Chapman and Hall, London, 1971).
9. A. G. GAYDON and I. R. HURLE, "The Shock Tube in High Temperature Chemical Physics" (Chapman and Hall, London, 1963).
10. I. I. GLASS and J. G. HALL, "Handbook of Supersonic Aerodynamics", Section 18, Shock Tubes, Navard Report, vol 6 (1959) 1488.
11. J. L. STOLLERY (Ed), "Shock Tube Research", Paper 60 (Chapman and Hall, London, 1971).
12. P. J. NURSE and P. E. REED, to be published.
13. E. H. ANDREWS, "Fracture in Polymers", Chapter 5 (Oliver and Boyd, Edinburgh, 1968).
14. E. S. FOLIAS, *Int. J. Fracture Mech.* **1** (1965) 104.
15. G. P. MARSHALL and J. G. WILLIAMS, *J. Mater. Sci.* **8** (1973) 138.

Received 30 March and accepted 13 July 1973.